Leonardo S. Vieira
DTE,
Electric Power Research Center (CEPEL),
Avenida Hum s/n,
CP 68007,
Cidade Universitária,
Rio de Janeiro 21944-970, Brazil
e-mail: lsrv@cepel.br

Carlos F. Matt
DIE,
Electric Power Research Center (CEPEL),
Avenida Hum s/n,
CP 68007,
Cidade Universitária,
Rio de Janeiro 21944-970, Brazil
e-mail: cfmatt@cepel.br

Vanessa G. Guedes
DTE,
Electric Power Research Center (CEPEL),
Avenida Hum s/n,
CP 68007,
Cidade Universitária,
Rio de Janeiro 21944-970, Brazil
e-mail: vanessag@cepel.br

Manuel E. Cruz
DEM/Politécnica/COPPE,
Federal University of Rio de Janeiro (UFRJ),
CT, CP 68503,
Cidade Universitária,
Rio de Janeiro 21945-970, Brazil
e-mail: manuel@mecanica.coppe.ufrj.br

Fernando V. Castellões
Petrobras R&D Center,
CENPES, Gas & Energy,
Avenida Horácio Macedo 950,
Cidade Universitária,
Rio de Janeiro 21941-915, Brazil
e-mail: fcastelloes@petrobras.com.br

Maximization of the Profit of a Complex Combined-Cycle Cogeneration Plant Using a Professional Process Simulator

The high cost of energy resources has driven a strong and continued quest for their optimal utilization. In this context, modern thermoeconomic optimization techniques have been developed to analyze and design improved energy systems, leading to a better compromise between energetic efficiency and cost. Thermoeconomic optimization can be parametric (plant configuration is fixed), applicable both at the design phase or operation phase of a system, or structural (plant configuration may vary). In practice, mathematical thermoeconomic optimization may be accomplished in two ways: (i) the conventional way, which manipulates all pertinent equations simultaneously or (ii) integrated with a professional process simulator, such that the equations are manipulated separately. In the latter case, the simulator deals with the thermodynamic property and balance equations, while an external optimization routine, linked to the simulator, deals with the economic equations and objective function. In this work, a previous implementation of an integrated approach for parametric mathematical thermoeconomic optimization of complex thermal systems is applied to an actual combined-cycle cogeneration plant located in the outskirts of the city of Rio de Janeiro in Brazil. The plant contains more than 60 thermal components, including two gas turbines, one steam turbine, and two heat recovery steam generators. Several hundred variables are required to simulate the plant at one operational steady-state. The plant produces 380 MW of power nominally, and exports a mass flow rate between 200 tons/h and 400 tons/h of superheated process steam, at 45 bars and 404°C, to a neighboring refinery. The simulator is the THERMOFLEX *software, which interfaces with the Microsoft Excel program. The optimization routine is written in the Visual Basic for Applications language and is based on Powell's method. The cogeneration plant operates subjected to time-changing economic scenarios, because of varying fuel, electricity, and steam prices. Thus, to manage the plant, it is necessary to vary the operational state appropriately as the economic parameters change. For a prescribed economic scenario, previous work determined the minimum operational cost, when a fixed contracted hourly-rate of process steam was to be exported, while a variable amount of electrical power was produced. In this paper, a broader optimization problem is formulated and solved, for which the objective is to maximize the plant profit under different economic scenarios. It is shown that the optimal operating conditions depend on the economic parameters, and do not necessarily imply maximum efficiency. The integrated optimization approach proves effective, robust, and helpful for optimal plant management.* [DOI: 10.1115/1.3204506]

1 Introduction

Effective utilization of costly nonrenewable energy resources by power plants is one critical task for sustainable growth and has pushed the development of thermoeconomics. In particular, in Brazil, thermal power generation is becoming increasingly strategic, because irregular rainfall has been recently threatening domestic power supply by the traditional hydroelectric plants. Natural gas, due to its abundance in South America, has been the fuel of choice to run the majority of Brazilian thermal power plants.

Thermoeconomics started in the 1960s [1], when association of thermodynamic and economic concepts in order to improve efficiency and reduce environmental impacts of thermal systems formally began. In the 1980s and 1990s a more systematic approach was embraced, which established general definitions, principles, and techniques [2,3], and led to the development of new methodologies [1,4–7] and the conception of the benchmark problem CGAM [3,8]. In the past 10 years, the effort to perfect thermal systems and to reduce their environmental impacts has vigorously persisted, with modern developments and improvements of methodologies [9–19], applications [20–27], and benchmark problems (TADEUS [28] and MPCP [29]); critiques of presently available methods and their limitations are found in literature [18,19,30]. Today, thermoeconomic and exergoeconomic concepts and formalisms [2,3,31,32] can be used together with optimization techniques [33–35] to perform analysis and design of energy systems, leading to a better compromise between energetic efficiency and environmental impact on one hand, and cost on the other. To date, with a few recent exceptions [23,24], the optimization applications have considered relatively simple systems only.

The objective of this work is to apply a previous implementation of an integrated approach for parametric mathematical thermoeconomic optimization of complex thermal systems [23] to an actual combined-cycle cogeneration plant located in the outskirts of the city of Rio de Janeiro in Brazil [36,37]. In the parametric optimization exercises reported here, the plant configuration is fixed (number and interconnections of components are un-

Manuscript received January 24, 2009; final manuscript received June 16, 2009; published online January 15, 2010. Review conducted by Paolo Chiesa.

changed), and, furthermore, the sizes of the components are also fixed; therefore, only their operational settings are altered in the optimization exercises. As in Ref. [36], due to the complexity of the energy system analyzed, the optimization algorithm is integrated with a professional process simulator—here, the THERMOFLEX program [38]. Robust system simulation is an essential element for the success of the optimization task [24,35]. The current plant is well simulated in both design and off-design conditions. Integration is realized through a routine written in the Visual Basic for Applications (VBA) language, since a Microsoft Excel supplement does the communication between the optimization algorithm and the simulator. The optimization routine is based on Powell's direct search method [33,39,40]. Search methods are widely employed in optimization of thermal systems [35]. Powell's method does not require the calculation of derivatives of the objective function, and, starting from an initial point, it locates the extremum of a multivariable unconstrained function by successive unidimensional searches along a set of conjugate directions generated by the algorithm. When constraints are imposed, one may couple the algorithm to a penalty function method. Validations of the integrated approach with other simulators [15,23] and with the present one [41] have already been performed.

The cogeneration plant operates subjected to time-changing economic scenarios, because of varying fuel purchase prices, and electricity and steam sale prices. Thus, to manage the plant competently, it is necessary to vary the operational state optimally as the economic factors change. For a prescribed economic scenario, previous work [36] determined the minimum operational cost, when a fixed contracted hourly-rate of process steam was to be exported, while a variable amount of electrical power was produced. In this paper, a broader optimization problem is formulated and solved, for which the objective is to maximize the profit of the plant under different economic scenarios. It is now shown that the optimal operating conditions depend (nontrivially) on the economic parameters, and do not necessarily imply maximum efficiency. It should be noted, however, that in the present work the ambient temperature fluctuation effects on the gas turbines and combined-cycle performances have not been considered. Thus, the current procedure is static, adequate to a general optimization facing variable prices and steam export parameters. To effect real-time dynamic optimization, the ambient temperature must be fed at regular intervals to the models of the gas turbines and all other components influenced by the ambient state. The results of optimization exercises to maximize the plant profit under various economic scenarios establish that the integrated optimization approach is effective, robust, and helpful for optimal plant management.

2 The Combined-Cycle Plant

The combined-cycle cogeneration plant of this study [36,37] is part of the largest natural-gas-fired thermoelectric complex in Brazil, located in the outskirts of the city of Rio de Janeiro. Main plant information has been provided by plant personnel [37] and is summarized in Table 1. Superheated process steam is exported to a neighboring refinery at 45 bars absolute pressure and 404°C temperature, with a mass flow rate between 200 tons/h (55.6 kg/s) and 400 tons/h (111.1 kg/s). The natural gas burned in the plant has the composition and properties presented in Table 2. An official performance test at design conditions indicated 382.1 MW net power, 5897 kJ/kWh cogeneration heat rate, and 201.4 tons/h process steam flow rate. At design conditions, the reference operational characteristics of the plant [37] are shown in Table 3. The basic components of the plant are briefly described next, and a schematic flow diagram is shown in Fig. 1.

Two gas turbines (GTs) operate in parallel with two supplemental duct burners (DBs) and two single-pressure heat recovery steam generators (HRSGs). The duct burners can nearly double steam production, and their operational settings depend on the amount of exported steam. In each HRSG, hot combustion gases flow outside the water-tubes of two superheaters, one evaporator, and two economizers, exiting through the chimney.

To make up for the exported mass flow rate of steam to the refinery (RE), demineralized water tanks feed the water/steam circuit of the plant. Water is preheated in the feedwater heater (FWH), follows to the deaerator (DE), and then enters the high pressure pumps (HPP). The water exiting from the pumps flows through the tube side of each HRSG and first gains energy in the economizers. Saturated steam is then formed in the evaporator and follows to the first superheater. To better control steam exit conditions, the steam undergoes attemperation before entering the

Table 1 Main combined-cycle plant information

Plant quantity	Value
Maximum net electrical power	383.2 MW
Auxiliary equipment power consumption	10 MW
Power of a gas turbine at full load	107.2 MW
Temperature of gases at inlet to HRSG after supplemental firing	795°C
HRSG design conditions for steam production	124.1 bars, 568°C
Exit temperature of gases from HRSG	112°C
Volume flow rate of combustion gases in HRSG	2,107,682 m^3/h
Hot gases total pressure loss in HRSG	27 mbars
Steam turbine power at full load (200 tons/h process steam)	179.3 MW
Steam conditions after first stage (200 tons/h process steam)	45.2 bars, 417°C

Table 2 Chemical composition and properties of the plant fuel (natural gas)

Chemical component	Molar fraction
Methane	87.9589%
Ethane	9.1950%
Propane	1.4882%
Butane	0.1667%
Pentane	0.016%
Hexane	0.0018%
Nitrogen	0.7064%
Carbon dioxide	0.4671%
Hydrogen	0
Hydrogen sulfide	0
Total	100%
Density (absolute)	0.7520 kg/m^3
Mean molecular weight	18.05
Lower heating value (LHV)	48,366 kJ/kg
Higher heating value (HHV)	53,522 kJ/kg

Table 3 Reference operational characteristics of the plant at design conditions: 200 tons/h exported steam and 100% GT load

Flow	P (bar)	T (°C)	h (kJ/kg)	$\dot{m}$ (kg/s)
Water entering HRSGs	156.4	82.1	356.2	95.1
Superheated steam exiting HRSGs	124.1	567.4	3519.8	95.1
Combustion gases exiting GTs	1.03	540.3	591.1	385.6
Combustion gases exiting DBs	1.01	795.0	907.0	388.1
Combustion gases exiting HRSGs	1.01	112.3	119.1	388.1
Steam entering first stage of ST	120.0	565.0	3517.7	190.2
Steam exiting last stage of ST	0.08	41.0	2239.1	122.0
Water exiting condenser	0.08	41.0	171.8	122.0
Water exiting low-pressure pump	6.0	41.1	172.5	122.0
Water entering DE	0.47	41.2	172.5	122.0
Process steam after attemperation	45.2	404.3	3217.0	55.6

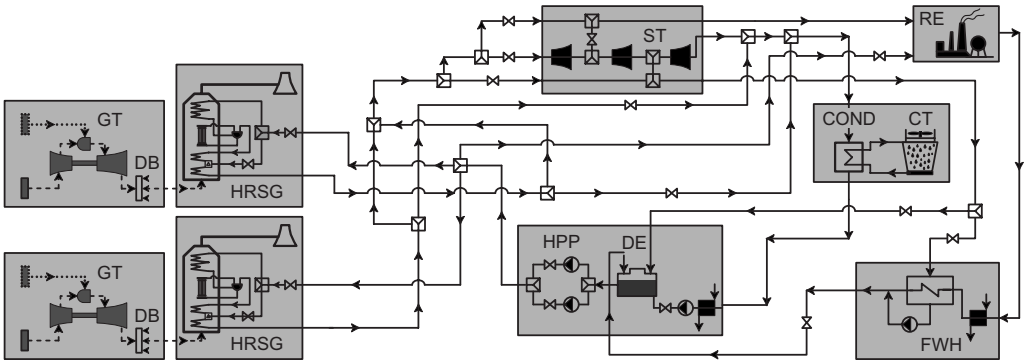

Fig. 1 Schematic flow diagram of the combined-cycle cogeneration plant

second superheater. The total amount of superheated steam produced in the HRSGs follows to the first stage of the steam turbine (ST) in normal operating conditions.

The condensation steam turbine is designed for sliding pressure operation. After expansion in the first stage, some amount of steam is extracted to serve the process line (after undergoing attemperation). In turn, after expansion in the second stage, more steam is extracted to serve the deaerator. Finally, after expansion in the third twin-stage, steam follows to the water-cooled condenser. The condenser receives cooling water at 25°C from a humid forced-convection cooling tower (CT), and the water leaves at 37.1°C. A low-pressure pump directs the condensate to the deaerator. The hot stream of the feedwater heater is steam, which had been deviated from the first and third stages of the steam turbine. Several valves (blockage and control), mixers, and splitters are used throughout the system to direct, join, and separate the various mass flows.

3 The Thermoflex Simulator

Process simulators are useful modern engineering tools for the design, analysis, and optimization of thermal systems [23,24,42]. As alluded to before, the concerted effort to attain robust plant simulation, though time consuming, is indispensable for the success of the optimization task [24,35]. The THERMOFLEX process simulator is the fully-flexible program of Thermoflow, Inc [38]. In this work, version 16.0.1 has been used.

Along an optimization process (e.g., operation cost minimization or profit maximization) of an energy system modeled in a simulator, it is necessary to simulate the system in conditions away from those, for which it had been designed. For this purpose, the system must then be modeled in off-design mode of the program. However, to build the off-design model, it is first necessary to build the design model in design mode. The components and their interconnections are exactly the same for both models; Fig. 2 shows the flow diagram for the off-design model. The ambient parameters have been set to $T_{amb}=22°C$, $P_{amb}=1.0132$ bars, and 75% relative humidity [36]. In both design and off-design models of the plant, the account of pressure losses in the pipelines has not been considered relevant for the present optimization problem [37].

3.1 The Design Model. In order to contemplate all the main specifications and features of the combined-cycle plant, the following THERMOFLEX components have been selected to build the design model [36]: four fuel sources, two gas turbines (GTPRO), five gas/air sources, three gas/air sinks, four economizers (PCE), two evaporators (PCE), four superheaters (PCE), two stacks, two desuperheaters (attemperators), two supplemental duct burners, three steam turbines to play the role of the three expansion stages of the actual turbine, one water-cooled condenser, one wet cooling tower (PCE), one deaerator, one feed water heater with pump, one auxiliary water pump, two high-pressure water pumps, two makeup water sources makeup/blowdown, necessary to satisfy the mass balances for the closed water circuits, eleven flow splitters, six flow mixers, one element process with return, seventeen valves for flow blockage and control, one water/steam sink, and one water/steam source. Additionally, several simulator features (e.g., "fix a flow" and "fix a pressure" settings in various dialog boxes) have had to be used to impose all the plant constraints (see Sec. 6.1).

Clearly, the plant is complex. There are a total of 79 simulator components, with many interconnections. The flow paths for the fluid circuits are shown with solid (water/steam), dotted (fuel), and dashed (gases) lines. All the options for steam bypass and extraction to supply the process line, the deaerator, and the water heat exchanger are considered in the model; in this work, however, the exported process steam is always expanded in the first stage of the steam turbine. To calculate the exergies of the various system flows, the same reference flows defined in Ref. [36] are used. The main input data for the design model to simulate the plant in design conditions, with the exported process steam mass flow rate of 200 tons/h and 100% load in the gas turbines, are shown in Table 4.

3.1.1 Validation of the Design Model. Simulating the design model described in Sec. 3.1 with the input data specified for design conditions in Table 4, with the exported steam mass flow rate of 200 tons/h and 100% load in the GTs, the results obtained are within a maximum of 2.8% of the reference operational values of Table 3; gross plant power and heat rate are predicted to within 0.8% and 1.2%, respectively [37]. The magnitudes of these relative deviations are compatible with normally verified simulations deviations (1–5%) in other recent studies in literature [22,43,44], and are thus considered acceptable for the present purposes.

3.2 The Off-Design Model. In the off-design model, all the components present in the design model are switched from design mode to off-design mode, except for the cooling tower (for which the off-design model is not available in the simulator version used [38]). As shown in the flow diagram of Fig. 2, there are a total of 102 mass flow rates and 79 simulator components; however, only 62 are actual thermal components of the system to be subjected to analysis and optimization (17 are sources/sinks). Some component and stream options in the off-design model have to be changed relative to those in the design model, so as to permit proper simulation of the plant exporting different amounts of process steam. Finally, the input data for the off-design model are not identical to those for the design model.

In the simulator model, the off design mode regards the gas turbines, the HRSGs, and the steam turbine. The gas turbines may operate at partial loads from 60% to 100%. The HRSGs produce variable amounts of steam as the GT loads change. The steam turbine model incorporates sliding pressure operation and variable mass flow rate of steam through the expansion stages. It is important to note that the model accounts for the decrease in the isen-

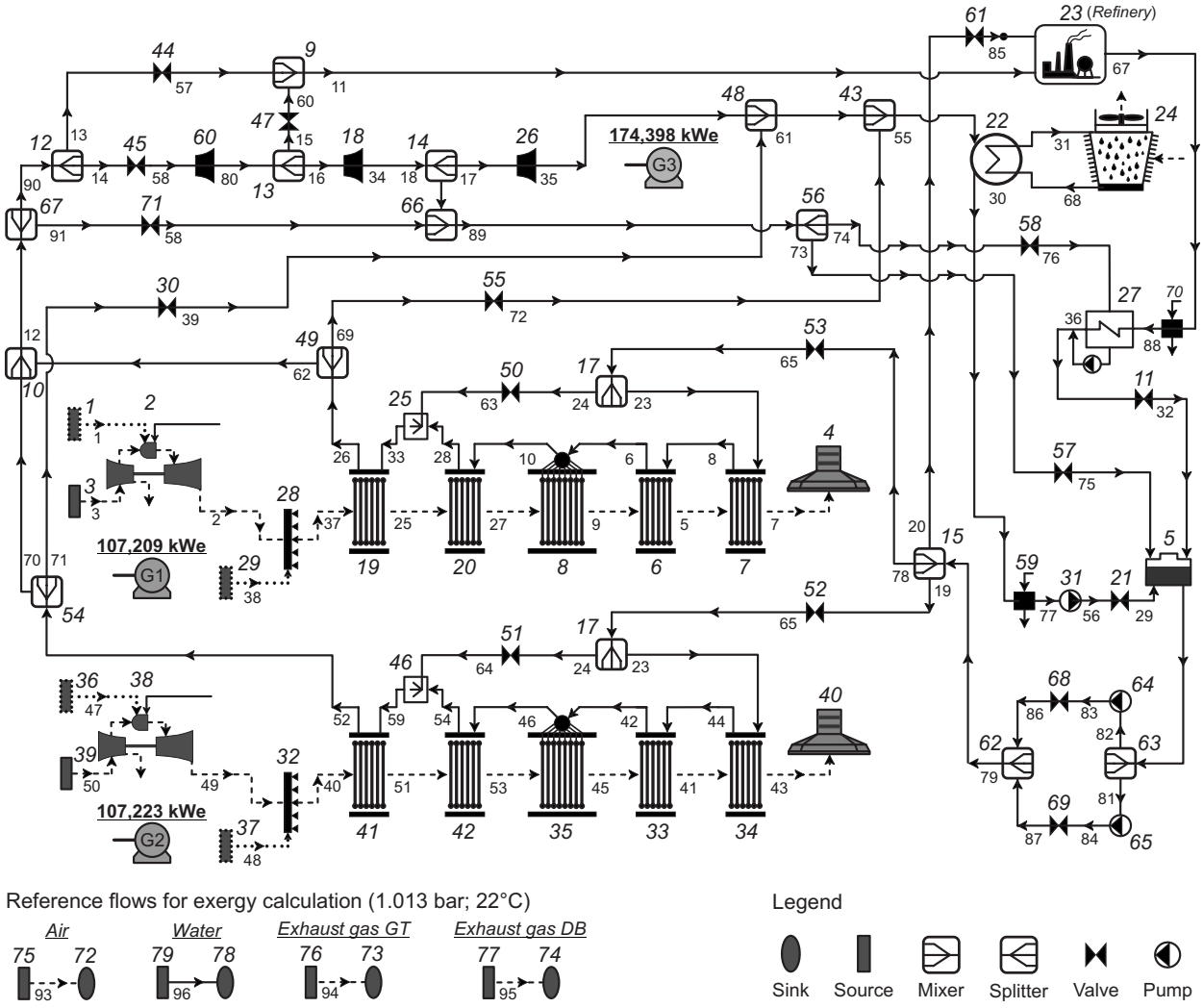

Fig. 2 Schematic flow diagram of the off-design model for the plant (component numbers are italicized, flow numbers appear in normal font)

tropic efficiency of a stage as the mass flow rate of steam through it increases. In fact, the efficiency of the low-pressure stage is 0.86 at the minimum of 13 kg/s of steam, while it is 0.81 at 150 kg/s; roughly, this 6% drop occurs linearly. In turn, the low-pressure stage power production varies linearly with the isentropic efficiency, and it represents about 15% of the total plant power production. Therefore, the effect of the variation in the stage isentropic efficiency on the total power production is not major, but still accounted for in the simulations along the optimization processes.

3.2.1 Validation of the Off-Design Model. First, simulating the off-design model for design conditions (200 tons/h), the results obtained are within 0.5% of those generated with the design model [36]. More importantly, results of plant simulations at off-design operational conditions (100 tons/h and 400 tons/h) have been validated by plant personnel in the light of real operational data for global quantities and thermodynamic flow variables [37]. As a matter of fact, Table 5 shows key global simulation results of the off-design model for exported process steam flow rates of 100

Table 4 Main input data for the design model

Design model quantity	Value
Pressure and temperature of process steam	45 bars, 404°C
Steam pressure at the inlet to the first stage	120 bars
Temperature of gases at the exit from the supplemental duct burners	795°C
Steam temperature and pressure loss at the exit from the first economizer	300.1°C, 1% of inlet pressure
Steam temperature and pressure loss at the exit from the second economizer	329.5°C, 1% of inlet pressure
Steam temperature and pressure loss at the exit from the first superheater	416.9°C, 1% of inlet pressure
Steam temperature and pressure loss at the exit from the second superheater	567.9°C, 1% of inlet pressure
Steam mass flow rate through the evaporators	92.8 kg/s
Pressure loss of gases in the economizers and superheaters	2.491 mbars
Pressure loss of gases in the evaporators	4.981 mbars

Table 5 Global simulation results of the off-design model for exported process steam mass flow rates of 100 tons/h, 200 tons/h, and 400 tons/h, and 100% GT load

Off-design simulator model			
Global result	100 tons/h	200 tons/h	400 tons/h
Gross power of GTs (kW)	214,432	214,432	214,432
Gross power of ST (kW)	202,401	174,398	118,422
Gross power of the plant (kW)	416,833	388,830	332,854
Fuel consumption based on LHV (kW)	907,855	907,855	907,855
Electrical efficiency based on LHV (%)	45.9	42.8	36.7
Auxiliary consumption (kW)	11,387	11,312	11,165
Net power of the plant (kW)	405,446	377,518	321,689
Net electrical efficiency based on LHV (%)	44.7	41.6	35.4
Net heat rate based on LHV (kJ/kWh)	8,061	8,657	10,160
Energy extraction for process (kW)	85,228	170,455	340,910
Energy efficiency of cogeneration based on LHV (%)	54.1	60.4	73.0

tons/h, 200 tons/h, and 400 tons/h, and 100% GT load. The results in Table 5 translate with fidelity the global behavior of the plant; thermodynamic variables of the plant flows are further verified in Ref. [37]. It is observed that, as the exported steam increases, the electrical power production and the associated efficiency decrease, but the cogeneration energy efficiency increases.

The simulations results presented in Secs. 3.1 and 3.2 indicate that both the design and off-design models constructed in the simulator reproduce with engineering accuracy the most relevant cogeneration plant operational quantities. This is crucial to parametrically optimize an objective function for a power plant, as the optimization process leads to operational adjustments both of macroparameters (such as load and fuel input) and model-internal variables (such as flow rates and thermodynamical properties). It is thus expected that the off-design model developed will be appropriate for the optimization purposes of this work.

4 The Economic Model

In general, the costs of a thermal system include the capital investment, supplied resources (fuel, electricity, and streams), and operation and maintenance costs [3]. In this work, it has not been judged of interest to consider the investment and operation and maintenance costs of the actual cogeneration plant [36,37]. Thus, the total cost of the plant on a rate basis, $\dot{C}_T$, is formed by the consumption costs of natural gas and other resources only, or

$$\dot{C}_T = \dot{C}_f + \dot{C}_{other} = c_f \dot{m}_f \mathrm{LHV} + \dot{C}_{other} \quad (1)$$

where c_f, $\dot{m}_f$, and LHV are, respectively, the cost per unit exergy, the mass flow rate, and the lower heating value (assumed equal to the chemical exergy) of the fuel, and $\dot{C}_{other}$ is the cost rate of the other resources.

Market fluctuations force the cogeneration plant to operate subjected to time-changing economic scenarios, because of varying fuel, electricity, and steam prices. The plant buys natural gas and sells electricity to the distribution network at the price commonly referred to as the difference marketable price in Brazil, henceforth, abbreviated as DMP. Also, the plant sells superheated steam to a neighboring refinery at variable prices per unit mass. In this work, an effort is made to reflect reality by considering six (discrete) economic scenarios. The different combinations of values of the DMP, and fuel and steam prices for the investigated scenarios are indicated in Table 6. The prices in Table 6 have been judiciously established by plant personnel after an economic study [37] and represent limiting values, which are possible to occur in the Brazilian energy market.

In the flow diagram of Fig. 2, there are a total of 12 external flows entering the plant, of which fuel gas and power only are assumed to imply some costs; electricity consumed internally, at an estimated price of 60.00 US $/MWh, and natural gas to the gas turbines and duct burners, priced at the values shown in Table 6. Note that the plant is part of a single-company industrial complex, and it is not charged for the demineralized water.

5 Exergoeconomic Analysis of the Plant

An exergoeconomic analysis can be performed, integrated with the simulator program, at an operational point **X** of the cogeneration plant [36,37]. Here, a point of operation **X** refers to the steady-state operation of the plant corresponding to one particular set of values assigned to the decision variables of the optimization problem (see Sec. 6). To effect optimization of a thermal system, it is necessary to select an initial set of estimates for the decision variables, which will correspond to the initial point $\mathbf{X}_0$. At the end of the optimization process, a final point $\mathbf{X}_f$ is obtained. Therefore, by comparing the exergoeconomic analyses for the initial and final points, the modifications realized on the system by the optimization process can be readily appreciated.

The calculations involved in an exergoeconomic analysis are presented in Refs. [1,3,7,15,18,23], and they have been outlined in Refs. [36,37] for the current plant. Because THERMOFLEX (version 16.0.1) does not supply the flow exergy of a stream directly, it has been calculated in an external routine, using the values of the other thermodynamic properties, and taking the ambient conditions as reference. Detailed quantitative results of exergoeconomic analyses of the plant are reported in Ref. [37]; an excerpt of the results is provided in Ref. [36].

6 Maximization of the Plant Profit

In the parametric thermoeconomic optimization of the plant effected here, structural changes in the design are not allowed, so that the configuration is fixed, shown in Figs. 1 and 2, and the component sizes are also fixed. Both of the gas turbines, the respective HRSGs, and the steam turbine are assumed to always operate. Only the operational settings of the plant equipment can be changed during the optimization procedure.

Table 6 Economic scenarios for the combined-cycle cogeneration plant of this work

Economic scenario	DMP (US $/MWh)	Fuel (US $/MBTU)	Fuel (US $/MWh)	Steam (US $/ton)
1	8.80	5.15	17.57	20.35
2	75.00	5.15	17.57	20.35
3	75.00	11.00	37.53	20.35
4	8.80	11.00	37.53	20.35
5	8.80	11.00	37.53	10.00
6	75.00	5.15	17.57	32.50

An optimization exercise consists of the application of the integrated iterative optimization approach to the off-design simulation model starting at an initial point of operation, with ensuing execution of the algorithm until a stopping criterion is satisfied, so that a final point of operation is obtained. The initial point is generically denoted by $\mathbf{X}_0$, and possesses an associated value of the objective function, OF_0. The point obtained at the end of the iterations, $\mathbf{X}_f$, contains the final values of the decision variables, and is associated with the final value OF_f; of course, OF_f is improved relative to OF_0. Indeed, one expects that $\mathbf{X}_f$ is close to, if not coincident with, the system global optimum point $\mathbf{X}^*$, associated with OF^*. In this work, two initial points are considered, denoted by $\mathbf{X}_{0,1}$ and $\mathbf{X}_{0,2}$, and they correspond, respectively, to full load and partial load operation of the gas turbines. By testing with different initial points, first, the likelihood of reaching the global minimum is increased [11], and second, the robustness of the integrated optimization approach may be verified.

6.1 Problem Formulation. In the literature [1,3,8,23], a typical optimization problem is to minimize the sum of the plant investment, operation and maintenance, and fuel costs. For the present cogeneration plant, however, the economic model equates the total cost rate of the system, $\dot{C}_T$, to the cost rate associated with the consumption of natural gas and other resources only, $\dot{C}_f + \dot{C}_{\text{other}}$ [36,37]. In this work, it has been found that $\dot{C}_{\text{other}}$ (here, the cost rate of the electricity consumed internally, priced at 60.00 US \$/MWh) has a negligible effect on the plant expenditures. Therefore, only $\dot{C}_f$ is considered in the optimization problem formulation.

The objective function to be maximized in the optimization problem is the plant profit, or the difference between the total plant revenue and the total cost of natural gas. The plant revenue is yielded by the electricity and steam sales, such that the objective function OF' (US \$/h) can be mathematically expressed by

$$OF' = \dot{P}_e \text{DMP} + \dot{m}_{\text{ps}} \Pi_{\text{ps}} - c_f \dot{m}_f \text{LHV} \tag{2}$$

where $\dot{P}_e$, $\dot{m}_{\text{ps}}$, and Π_{ps} represent, respectively, the net electrical power generated, the exported steam mass flow rate, and the steam sale price in US \$/ton. Note that $\dot{P}_e$ considers the electricity consumed internally. In this work, maximization of OF' is obtained equivalently through minimization of $OF = -OF'$, such that positive and negative values of OF correspond to plant loss and plant profit, respectively. Solution of the optimization problem is obtained for three exported steam mass flow rates, namely, 100 tons/h, 200 tons/h, and 400 tons/h.

It is remarked that the objective function OF is not equivalent to the specific cost of consumed resources for the plant. The latter has an inverse correlation with plant efficiency and has been minimized in Ref. [36]. The imparity between these objective functions arises, because the total plant revenue changes even for a fixed exported steam mass flow rate; note that $\dot{P}_e$ depends on the operational settings of the plant equipment. Therefore, depending on the economic scenario, the operational settings for maximum plant profit may not coincide with the ones for maximum plant efficiency (or, equivalently, minimum specific cost of resources).

6.1.1 Decision Variables. The set of decision variables has been selected after several preliminary tests [36,37] and consists of the following seven variables: loads of the gas turbines, ϕ_{GT2} and ϕ_{GT38}; fuel mass flow rates in the duct burners, $\dot{m}_{\text{DB28}}$ and $\dot{m}_{\text{DB32}}$; steam flow pressures in the evaporators, $P_{\text{Evap,10}}$ and $P_{\text{Evap,46}}$; and steam mass flow rate to the deaerator, $\dot{m}_{\text{DE,92}}$. While it is desired mathematically that the decision variables may be altered over a wide range of values, physical operational restrictions on the plant apparatuses must nevertheless be contemplated. The following upper and lower limits have been established to the decision variables [36,37]: $60\% \leq \phi_{\text{GT2}}$, $\phi_{\text{GT38}} \leq 100\%$, $0 \leq \dot{m}_{\text{DB28}}$, $\dot{m}_{\text{DB32}} \leq 3.0$ kg/s, 100 bars $\leq P_{\text{Evap,10}}$, $P_{\text{Evap,46}} \leq 150$ bars, and $0 \leq \dot{m}_{\text{DE,92}} \leq 60$ kg/s.

The steam mass flow rate in each HRSG is a strong function of the load of the respective GT. Thus, in addition to the GT loads, the pressure in the evaporator is the appropriate HRSG-related variable to be selected as a decision variable. In the simulator program [38], to make a pressure or a mass flow work as a decision variable, it is mandatory to use an option, which fixes the selected variable in an individual simulation. The sliding pressure mode of the steam turbine model accommodates the evaporator pressure variations from simulation to simulation along the iterations of one optimization exercise. The steam bypass to the deaerator serves as a useful check for the robustness of the optimization process, in that $\dot{m}_{\text{DE,92}}$ should converge to the minimum value possible.

6.1.2 Constraints. The mass and energy balances for the plant are equality constraints of the optimization problem, imposed by the thermodynamic calculations of the simulator. In addition, the fixed mass flow rate value of the exported process steam is also an equality constraint.

The inequality constraints of the optimization problem are presented in Tables 7 and 8 [36,37]. Some constraints are due to specific operational characteristics of the plant apparatuses, such

Table 7 Inequality constraints of the optimization problem

Description of constraint	Value
Lower limit for the power of each gas turbine	64.5 MW
Minimum steam mass flow rate through the low-pressure stage of the steam turbine	13 kg/s
Maximum temperature at the exit of the deaerator	81 °C
Minimum gas flow rate through the duct burners	2100 m^3/h
Maximum exit temperature of gases from the duct burners	795 °C
Minimum and maximum energy fluxes in the duct burners	24.9 MW, 124.3 MW
Minimum and maximum exit temperatures of gases from the HRSGs	100 °C, 200 °C
Maximum exit temperature of steam from the HRSGs	567 °C
Maximum pressure at the entrance to the HRSGs	229 bars
Minimum pressure in the high pressure pumps	161 bars
Minimum and maximum steam pressure at the entrance to the steam turbine	64 bars, 121 bars
Maximum condenser pressure	1.7 bars
Minimum and maximum process steam pressure	41.5 bars, 48 bars

Table 8 Upper limit for the steam temperature at the entrance to the steam turbine, as a function of the steam mass flow rate

Mass flow (kg/s)	Temperature (°C)
0	460
90	460
100	465
110	470
120	490
130	505
140	520
150	530
160	540
170	550
180	560
185	565
200	565

Table 9 Results for the first set of optimization exercises: exported steam mass flow rates of 100 tons/h, 200 tons/h, and 400 tons/h, economic scenario 1

Exported steam	Point	ϕ_{GT2} (%)	ϕ_{GT38} (%)	$\dot{m}_{DB28}$ (kg/s)	$\dot{m}_{DB32}$ (kg/s)	$P_{Evap,10}$ (bar)	$P_{Evap,46}$ (bar)	$\dot{m}_{DE,92}$ (kg/s)	OF (US $/h)	N_C
100 tons/h	$\mathbf{X}_{0,1}$	100	100	2.54	2.54	129.5	129.5	5.56	10,374.10	1
	$\mathbf{X}_{f,1}$	60	60	1.16	1.13	117.0	119.5	0.0087	6,343.75	291
200 tons/h	$\mathbf{X}_{0,1}$	100	100	2.54	2.54	129.5	129.5	5.56	8,585.16	1
	$\mathbf{X}_{f,1}$	60	60	1.16	1.17	117.0	117.0	0.0087	4,585.18	252
400 tons/h	$\mathbf{X}_{0,1}$	100	100	2.54	2.54	129.5	129.5	5.56	5,006.93	1
	$\mathbf{X}_{f,1}$	60	60	1.24	1.25	150.0	148.9	0.0087	1,104.70	579
100 tons/h	$\mathbf{X}_{0,2}$	75	75	1.50	1.50	129.5	129.5	5.00	7,665.62	1
	$\mathbf{X}_{f,2}$	60	60	1.08	1.10	121.7	120.8	0.050	6,284.17	301
200 tons/h	$\mathbf{X}_{0,2}$	75	75	1.50	1.50	129.5	129.5	5.00	5,878.28	1
	$\mathbf{X}_{f,2}$	60	60	1.10	1.10	121.6	120.8	0.050	4,504.15	187
400 tons/h	$\mathbf{X}_{0,2}$	75	75	1.50	1.50	129.5	129.5	5.00	2,292.42	1
	$\mathbf{X}_{f,2}$	62	63	1.15	1.28	135.4	149.8	0.53	1,191.45	546

as the pressure in the high pressure pumps and the exit temperature of gases from the duct burners. Other constraints originate from established engineering practices, such as the exit temperatures of gases from the HRSGs. Minimum values equal to zero, that would represent structural changes of the system, have been avoided; such is the case for the mass flow rate in the duct burners and in the turbines.

As commonly employed in direct search optimization algorithms [23,33,35], the inequality constraints are incorporated through penalties applied to the objective function. Here, a penalty increases the objective function OF by a very large amount, which is proportional to the magnitude of the difference between the current (not admissible) value of the constrained variable and the respective limiting value.

6.2 Method of Solution. The formulated thermoeconomic optimization problem is solved by integrating a direct search optimization algorithm with the process simulator [36]. Integration requires a two-way communication interface, provided by the Microsoft Excel supplement ELINK [38]. The optimization routine is written in the VBA language, runs without user intervention, and performs the following tasks: (i) send plant data to the THERMOFLEX process simulator, (ii) issue the command to run a simulation ("call *MnuCompute*"), (iii) receive new plant data from the simulator, (iv) effect calculations of the algorithm, and (v) return to task (i), while the stopping criterion is not met. The associated computer code has been described in Refs. [36,37]; the enthalpy and entropy of the fuel are calculated using an external .xla routine from the supplement FLUIDPROP [45].

In Ref. [23], Nelder and Mead's method [33] had been implemented and integrated with the IPSEPRO simulator [46]. However, separate tests conducted with the Nelder and Mead method applied to the cogeneration plant modeled in the current program revealed that the method demanded a very long computational time to realize one optimization exercise [36,37]. In view of this experience, it has been decided to replace Nelder and Mead's method by the method of Powell [33,39], as implemented in Ref. [40].

In Ref. [40], Powell's method is implemented in VBA, integrated with the IPSEPRO simulator. In multidimensional optimization, the method requires a one-dimensional search for the function extremum in each coordinate direction. To perform this search efficiently, the combined DSC-Powell algorithm [33] has been used. Validation of the implementation is obtained through standard functions and against the results of Ref. [23] for the same energy system and operating conditions. In this work, the implementation of Ref. [40] is modified, so as to integrate it with THERMOFLEX. It is then observed [36,37] that the performance of Powell's method is about five times faster than that of the method by Nelder and Mead. Here, successive reinitializations of the algorithm are effected until the objective function ceases to reduce, according to the stopping criterion

$$|OF_{\text{iter}+1} - OF_{\text{iter}}| < \sigma \tag{3}$$

where iter+1 and iter represent consecutive iterations, and $\sigma = 10^{-2}$ is a prescribed tolerance suited for monetary quantities. No limit on the number of iterations has been imposed.

7 Results and Discussion

In this section, the results of the exercises to optimize the cogeneration plant profit are presented and analyzed. Note that, in accordance with the problem formulation, the results are presented in terms of the objective function OF (operation losses), not OF' (operation profit). Two sets of optimization exercises have been carried out. The first set has been performed for three values of the exported steam mass flow rate, 100 tons/h, 200 tons/h, and 400 tons/h, and for the economic scenario 1 only (see Table 6). Two initial points have been selected, $\mathbf{X}_{0,1}$ and $\mathbf{X}_{0,2}$, corresponding to full load and partial load operation of the gas turbines, respectively. The second set has been executed for the six economic scenarios indicated in Table 6; all exercises start from the point $\mathbf{X}_{0,1}$ and 200 tons/h is the exported steam mass flow rate.

7.1 Results for Several Exported Steam Mass Flow Rates. The results for the first set of optimization exercises are shown in Table 9 and Fig. 3. The number of calls to the simulator along the iterations of one optimization exercise is denoted by N_C, which is equal to the number of evaluations of the objective function. Evidently, larger values of N_C correspond to larger computational times; on a Pentium IV processor, $N_C = 150$ amounts roughly to 1 h.

From the results in Table 9 and Fig. 3 for the economic scenario 1, it is observed, first, that the algorithm is effective and robust: (i) plant losses at the final points are significantly reduced relative to those at the respective initial points and (ii) for each exported steam mass flow rate, the final value of OF is (acceptably) independent of the initial point. Second, the higher the amount of exported steam is, the lower is the loss. Third, both GTs must operate at the minimum load of 60%, regardless of the exported steam mass flow rate. This is a combined effect of cheap fuel and

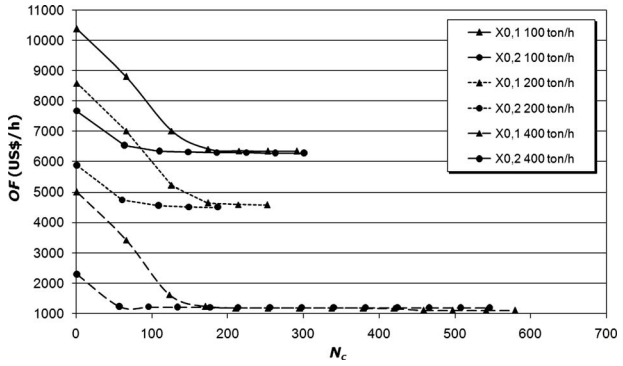

Fig. 3 Optimization results, *OF* versus N_C, for the first set of exercises

low DMP value; to minimize plant losses, it is better to minimize electricity production in the GTs and to keep some duct firing to guarantee steam export. Fourth, for all amounts of exported steam, the fuel mass flow rates in the duct burners must be reduced to values within the range from 1.1 kg/s to 1.3 kg/s. The reductions in the GT loads and in the amounts of fuel through the duct burners contribute to lower the temperature of the combustion gases. Fifth, the final values of the steam pressure in the evaporators are lower than the corresponding initial values, except for 400 tons/h. In this case, the pressure must be increased to reduce the demanded thermal energy to generate the amount of exported steam in the HRSGs. Sixth, at all the final points, the bypass steam mass flow rate to the deaerator is markedly reduced. Finally, concerning the number of simulator calls, the more the system deviates from design conditions (200 tons/h), the higher is the value of N_C.

Table 10 summarizes, for the first set of optimization exercises, the global plant data at the final point $\mathbf{X}_{f,1}$ for each exported steam mass flow rate. It is observed from Table 10, that both the first-law and second-law electrical efficiencies decrease as the amount of exported steam is increased. The former is slightly higher than the latter, because the fuel energy flux (based on the LHV) has a lower numerical value than the exergy flux of all plant incoming streams (fuel, water and air). However, because the exergy flux value for the process steam is much lower than the energy flux, the first-law cogeneration efficiency is significantly higher than the second-law cogeneration efficiency. Also, as the amount of exported steam increases from 100 tons/h to 400 tons/h, the rate of increase in the first-law cogeneration efficiency (from 54.0% to 82.7%) is much higher than that of the second-law efficiency (from 44.6% to 48.2% only). The attenuated variation in the second-law efficiency indicates that the thermodynamic quality (reversible work potential) associated with a much increased exported steam mass flow rate is not so larger than the electric power losses due to extraction. Thus, higher amounts of exported steam do not lead to a much more rational utilization of the natural gas. Finally, comparing the efficiencies shown in Table 10 with the ones obtained for the optimization problem in Ref. [36], one verifies that the operational condition for maximum plant profit does not coincide with that for maximum plant efficiency. Indeed, e.g., for 200 tons/h, the first-law net electrical efficiency and the second-law cogeneration efficiency decrease from 41.8% and 48.4% (at maximum plant efficiency), respectively, to 35.0% and 45.7% (at maximum plant profit) [37].

7.2 Results for Several Economic Scenarios. The results for the second set of optimization exercises are shown in Table 11 and Fig. 4. As expected, scenario 5 is the worst (lowest DMP and steam sale price, and highest fuel price); conversely, scenario 6 is the best (highest DMP and steam sale price, and lowest fuel price). The plant makes profit operating under scenarios 2 and 6 only (highest DMP and lowest fuel price). For scenarios 1, 3, 4, and 5, the larger losses are associated with expensive fuel (purchased at 11.00 US $/MBTU), while the lower losses are associated with either expensive electricity (sold at 75.00 US $/MWh) or cheap fuel (purchased at 5.15 US $/MBTU).

In the economic scenarios 2 and 6 (DMP=75.00 US $/MWh and fuel at 5.15 US $/MBTU), irrespective of the steam price, the gas turbines and duct burners must operate at full load to generate maximum electrical power and increase the plant revenue. Of course, the fuel cost also increases, nevertheless, not at as high a rate as the revenue. To minimize the plant loss in the economic scenario 3 (DMP=75.00 US $/MWh, fuel at 11.00 US $/MBTU), on the other hand, while the gas turbines must also operate at full load, the fuel mass flow rates through the duct burners must be reduced relative to the values for scenario 6. Finally, to minimize the plant losses in the economic scenarios 4 and 5 (lowest DMP and expensive fuel), the gas turbines must operate at the minimum load of 60%. Also, the fuel mass flow rates through the duct burners should be reduced to the minimum necessary to permit production of the exported steam. Referring to Fig. 4, one observes clearly that the DMP and the fuel price are the quantities, which affect more significantly the final value of the objective function. Finally, again, the more the system deviates from design conditions (i.e., gas turbines operate at the minimum load), the higher is the value of N_C.

Table 12 summarizes, for the second set of optimization exercises, the global plant data at the final point $\mathbf{X}_{f,1}$ for each of the economic scenarios 1, 2, and 3. It is observed from Table 12 that both the gross and net electrical powers are the largest for the economic scenario 2, which forces the gas turbines and duct burners to operate at full load. Consequently, both the first-law and second-law net electrical efficiencies are the largest for scenario 2. It is also verified, that optimal plant operation for maximum profit

Table 10 Global plant data at the final point $X_{f,1}$ for each exported steam mass flow rate

	Economic scenario 1		
Plant data	100 tons/h	200 tons/h	400 tons/h
Gross electrical power (kW)	243,052	215,970	167,404
Net electrical power (kW)	235,688	208,527	159,798
Fuel consumption based on LHV (kW)	593,936	596,119	605,290
Process steam energy rate (kW)	85,241	170,483	340,845
First-law gross electrical efficiency (%)	40.9	36.2	27.7
First-law net electrical efficiency (%)	39.7	35.0	26.4
First-law cogeneration efficiency (%)	54.0	63.6	82.7
Total exergy flow rate of resources (kW)	605,876	608,187	617,659
Total exergy flow rate of process steam (kW)	34,658	69,345	137,634
Second-law net electrical efficiency (%)	38.9	34.3	25.9
Second-law cogeneration efficiency (%)	44.6	45.7	48.2

Table 11 Results for the second set of optimization exercises: economic scenarios 1–6 and exported steam mass flow rate of 200 tons/h

Economic scenario	Point	ϕ_{GT2} (%)	ϕ_{GT38} (%)	$\dot{m}_{DB28}$ (kg/s)	$\dot{m}_{DB32}$ (kg/s)	$P_{Evap,10}$ (bar)	$P_{Evap,46}$ (bar)	$\dot{m}_{DE,92}$ (kg/s)	OF (US $/h)	N_C
1	$\mathbf{X}_{0,1}$	100	100	2.54	2.54	129.5	129.5	5.56	8,585.16	1
	$\mathbf{X}_{f,1}$	60	60	1.16	1.17	117.0	117.0	0.0087	4,585.18	252
2	$\mathbf{X}_{0,1}$	100	100	2.54	2.54	129.5	129.5	5.56	−17,158.07	1
	$\mathbf{X}_{f,1}$	100	100	2.53	2.54	128.0	128.7	3.29	−17,315.29	194
3	$\mathbf{X}_{0,1}$	100	100	2.54	2.54	129.5	129.5	5.56	1,101.48	1
	$\mathbf{X}_{f,1}$	100	100	2.08	1.96	115.8	115.8	3.31	875.46	132
4	$\mathbf{X}_{0,1}$	100	100	2.54	2.54	129.5	129.5	5.56	26,844.70	1
	$\mathbf{X}_{f,1}$	60	60	1.16	1.17	117.0	117.0	0.0087	16,574.83	290
5	$\mathbf{X}_{0,1}$	100	100	2.54	2.54	129.5	129.5	5.56	28,914.87	1
	$\mathbf{X}_{f,1}$	60	60	1.16	1.17	117.0	117.0	0.0087	18,644.99	290
6	$\mathbf{X}_{0,1}$	100	100	2.54	2.54	129.5	129.5	5.56	−19,588.26	1
	$\mathbf{X}_{f,1}$	100	100	2.53	2.54	128.0	128.7	3.29	−19,745.48	195

(or minimum loss) leads to similar values of the first-law cogeneration efficiencies for all three scenarios; the same is true for the second-law cogeneration efficiencies. The lowest value of the second-law cogeneration efficiency occurs when the gas turbines operate at partial load, under scenario 1. Notwithstanding, for this scenario, the first-law cogeneration efficiency is the highest.

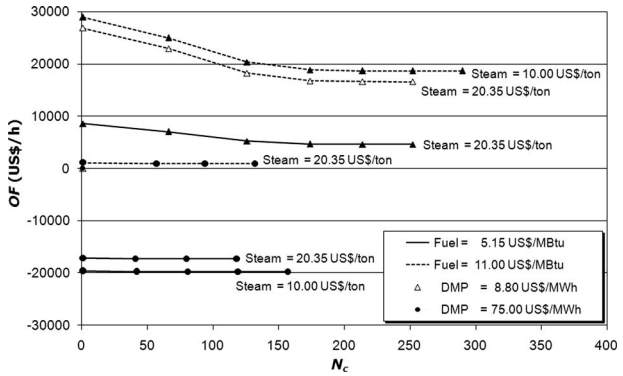

Fig. 4 Optimization results, *OF* versus N_C, for the second set of exercises

8 Conclusions

To conclude, this paper reports the successful integrated thermoeconomic optimization of the profit of a complex combined-cycle cogeneration plant operating subject to several different economic scenarios, using the THERMOFLEX professional process simulator. The efficient direct search optimization algorithm is based on the method of Powell. Optimization exercises with seven decision variables have been carried out for three exported steam mass flow rates (100 tons/h, 200 tons/h, and 400 tons/h) and they lead to a progressive improvement of the objective function. The integrated approach has proven effective, robust, and helpful for optimal plant management. Truly, in a dynamic economic setting, the approach can provide quantitative decision-making information that cannot be reliably anticipated.

Specifically, the results of the exercises show that the optimal plant operating conditions depend nontrivially on the economic parameters. Furthermore, the results conduct to some relevant conclusions: (i) maximization of the plant profit does not necessarily lead to the operating conditions of maximum plant efficiency (ii) as the exported steam mass flow rate is increased in an economic scenario with low DMP, the plant loss decreases; (iii) in an economic scenario with high DMP, maximization of the plant profit demands that the gas turbines operate at full load, while the load of the duct burners will depend on the fuel price; and (iv) in

Table 12 Global plant data at the final point $\mathbf{X}_{f,1}$ for each of the economic scenarios 1, 2, and 3

	Exported steam flow rate: 200 tons/h		
Plant information	Scenario 1	Scenario 2	Scenario 3
Gross electrical power (kW)	215,970	390,781	366,098
Net electrical power (kW)	208,527	382,277	357,853
Fuel consumption based on LHV (kW)	596,119	907,261	856,824
Process steam energy rate (kW)	170,483	170,455	170,454
First-law gross electrical efficiency (%)	36.2	43.1	42.7
First-law net electrical efficiency (%)	35.0	42.1	41.8
First-law cogeneration efficiency (%)	63.6	60.9	61.7
Total exergy flow rate of resources (kW)	608,187	922,766	871,686
Total exergy flow rate of process steam (kW)	69,345	68,793	68,895
Second-law net electrical efficiency (%)	34.3	41.4	41.1
Second-law cogeneration efficiency (%)	45.7	48.9	49.0

an economic scenario with low DMP, minimization of the plant loss demands that the gas turbines and duct burners operate at the minimum load possible.

Acknowledgment

M.E.C. thanks CNPq (Grant Nos. PQ-306592/2006-1 and APQ-472408/2007-0) and FAPERJ (Grant Bolsa Cientista do Nosso Estado, Grant No. E-26/152.694/2006) for financial support. The authors are very grateful to the reviewers for their many helpful comments and to Engineer Toseli Matos for his assistance with the figures.

Nomenclature

$\dot{C}_T$ = total cost rate of the plant (US \$/s or US \$/h)
c_f = cost per unit exergy of the fuel (US \$/kJ)
h = enthalpy (kJ/kg)
$\dot{m}$ = mass flow rate (kg/s)
$\dot{m}_{ps}$ = exported process steam mass flow rate (kg/s or ton/h)
$\dot{m}_f$ = fuel mass flow rate (kg/s or kg/h)
N_C = number of calls to the simulator
OF = objective function (US \$/h)
P = pressure (bar)
$\dot{P}_e$ = net electrical power generated by the plant (MW)
P_{Evap} = steam pressure in evaporator (bar)
T = temperature (°C)
$\mathbf{X}$ = steady-state operation point of the plant, vector of decision variables
Π_{ps} = process steam sale price (U S \$/ton)
ϕ = gas turbine load
σ = prescribed tolerance for optimization algorithm

References

[1] Tsatsaronis, G., 1993, "Thermoeconomic Analysis and Optimization of Energy Systems," Prog. Energy Combust. Sci., **19**(3), pp. 227–257.
[2] Kotas, T. J., 1985, *The Exergy Method of Thermal Plant Analysis*, Butterworth-Heinemann Ltd., Boston, MA.
[3] Bejan, A., Tsatsaronis, G., and Moran, M., 1996, *Thermal Design and Optimization*, Wiley, New York.
[4] Frangopoulos, C. A., 1983, "Thermoeconomic Functional Analysis: A Method for Optimal Design or Improvement of Complex Thermal Systems," Ph.D. thesis, Georgia Institute of Technology, Atlanta, GA.
[5] El-Sayed, Y. M., 1996, "A Second-Law-Based Optimization: Part 1—Methodology," ASME J. Eng. Gas Turbines Power, **118**(4), pp. 693–697.
[6] El-Sayed, Y. M., 1996, "A Second-Law-Based Optimization: Part 2—Application," ASME J. Eng. Gas Turbines Power, **118**(4), pp. 698–703.
[7] Lozano, M. A., and Valero, A., 1993, "Theory of the Exergetic Cost," Energy, **18**(9), pp. 939–960.
[8] Tsatsaronis, G., 1994, "Special Issue, Invited Papers on Exergoeconomics," Int J. Energy, **19**(3), pp. 279–381.
[9] Kwon, Y.-H., Kwak, H.-Y., and Oh, S.-D., 2001, "Exergoeconomic Analysis of Gas Turbine Cogeneration Systems," Int. J. Exergy, **1**(1), pp. 31–40.
[10] Tsatsaronis, G., and Park, M.-H., 2002, "On Avoidable and Unavoidable Exergy Destructions and Investment Costs in Thermal Systems," Energy Convers. Manage., **43**(9–12), pp. 1259–1270.
[11] Frangopoulos, C. A., 2003, "Methods of Energy Systems Optimization," OPTI_Energy Summer School, Gliwice, Poland.
[12] Rosen, M. A., and Dincer, I., 2003, "Exergy-Cost-Energy-Mass Analysis of Thermal Systems and Processes," Energy Convers. Manage., **44**(10), pp. 1633–1651.
[13] Cziesla, F., and Tsatsaronis, G., 2002, "Iterative Exergoeconomic Evaluation and Improvement of Thermal Power Plants Using Fuzzy Inference Systems," Energy Convers. Manage., **43**(9–12), pp. 1537–1548.
[14] Traverso, A., Massardo, A. F., Cazzola, W., and Lagorio, G., 2004, "WIDGET-TEMP: A Novel Web-Based Approach for Thermoeconomic Analysis and Optimization of Conventional and Innovative Cycles," ASME Paper No. 2004-GT-54115.
[15] Vieira, L. S., Donatelli, J. L., and Cruz, M. E., 2004, "Integration of an Iterative Methodology for Exergoeconomic Improvement of Thermal Systems With a Process Simulator," Energy Convers. Manage., **45**(15–16), pp. 2495–2523.
[16] Paulus, D. M., and Tsatsaronis, G., 2006, "Auxiliary Equations for the Determination of Specific Exergy Revenues," Energy, **31**(15), pp. 3235–3247.
[17] Milia, D., and Sciubba, E., 2006, "Exergy-Based Lumped Simulation of Complex Systems: An Interactive Analysis Tool," Energy, **31**(1), pp. 100–111.
[18] Lazzaretto, A., and Tsatsaronis, G., 2006, "SPECO: A Systematic and General Methodology for Calculating Efficiencies and Costs in Thermal Systems," Energy, **31**(8–9), pp. 1257–1289.
[19] Valero, A., 2006, "Exergy Accounting: Capabilities and Drawbacks," Energy, **31**(1), pp. 164–180.
[20] Alves, L. G., and Nebra, S. A., 2004, "Basic Chemically Recuperated Gas Turbines-Power Plant Optimization and Thermodynamics Second Law Analysis," Energy, **29**(12–15), pp. 2385–2395.
[21] Yokoyama, R., Takeuchi, S., and Ito, K., 2005, "Thermoeconomic Analysis and Optimization of a Gas Turbine Cogeneration Unit by a Systems Approach," ASME Paper No. GT2005-68392.
[22] Zhang, C., Wang, Y., Zheng, C., and Lou, X., 2006, "Exergy Cost Analysis of a Coal Fired Power Plant Based on Structural Theory of Thermoeconomics," Energy Convers. Manage., **47**(7–8), pp. 817–843.
[23] Vieira, L. S., Donatelli, J. L., and Cruz, M. E., 2006, "Mathematical Exergoeconomic Optimization of a Complex Cogeneration Plant Aided by a Professional Process Simulator," Appl. Therm. Eng., **26**(5–6), pp. 654–662.
[24] Koch, C., Cziesla, F., and Tsatsaronis, G., 2007, "Optimization of Combined Cycle Power Plants Using Evolutionary Algorithms," Chem. Eng. Process., **46**(11), pp. 1151–1159.
[25] Cardona, E., and Piacentino, A., 2007, "Optimal Design of CHCP Plants in the Civil Sector by Thermodynamics," Appl. Energy, **84**(7–8), pp. 729–748.
[26] Sanaye, S., and Ghazinejad, M., 2007, "Thermoeconomic Optimization of Gas Turbine Combined Heat and Power System in a Paper Mill," ASME Paper No. GT2007-27206.
[27] Borelli, S. J. S., and Junior, S. O., 2008, "Exergy-Based Method for Analyzing the Composition of the Electricity Cost Generated in Gas-Fired Combined Cycle Plants," Energy, **33**(2), pp. 153–162.
[28] Valero, A., Correas, L., Zaleta, A., Lazzaretto, A., Verda, V., Reini, M., and Rangel, V., 2004, "On the Thermoeconomic Approach to the Diagnosis of Energy System Malfunctions Part 1: The TADEUS Problem," Energy, **29**(12–15), pp. 1875–1887.
[29] Costa, A. N., and Cruz, M. E., 2008, "Solution of the Maximum Profit Cogeneration Plant (MPCP) Optimization Problem Using the Mathematica Program," *Proceedings of the 12th Brazilian Congress of Thermal Engineering and Sciences (ENCIT)*, Rio de Janeiro, Brazil, ABCM Paper No. 4-5475.
[30] Tsatsaronis, G., 2007, "Definitions and Nomenclature in Exergy Analysis and Exergoeconomics," Energy, **32**(4), pp. 249–253.
[31] El-Sayed, Y. M., 2003, *The Thermoeconomics of Energy Conversions*, Elsevier, Oxford.
[32] Dincer, I., and Rosen, M. A., 2007, *Exergy, Energy, Environment and Sustainable Development*, Elsevier, Oxford.
[33] Himmelblau, D. M., 1972, *Applied Nonlinear Programming*, McGraw-Hill, New York.
[34] Arora, J. S., 2004, *Introduction to Optimum Design*, 2nd ed., Elsevier, Amsterdam.
[35] Jaluria, Y., 2008, *Design and Optimization of Thermal Systems*, 2nd ed., CRC, Boca Raton, FL/Taylor & Francis, London.
[36] Vieira, L. S., Matt, C. F., Guedes, V. G., Cruz, M. E., and Castelloes, F. V., 2008, "Optimization of the Operation of a Complex Combined-Cycle Cogeneration Plant Using a Professional Process Simulator," ASME Paper No. IMECE2008-66717.
[37] Vieira, L. S., Guedes, V. G., Matt, C. F., and Cruz, M. E., 2008, "Application of an Exergoeconomic Optimization Methodology to Thermal Power Plants," CEPEL, Final Technical Report No. DTE-20048/08.
[38] Thermoflow, Inc., 2004, *Thermoflex, Fully-Flexible Heat Balance Engineering*, Thermoflow, Inc., Sudbury, MA.
[39] Powell, M. J. D., 1964, "An Efficient Method for Finding the Minimum of a Function of Several Variables Without Calculating Derivatives," Comput. J., **7**(2), pp. 155–162.
[40] Cordeiro, A. S., 2007, "Optimization and Exergoeconomic Improvement of Thermal Systems Modeled in a Process Simulator Using Direct Search and Stochastic Methods," M.Sc. thesis, PEM/COPPE/UFRJ, Rio de Janeiro, Brazil, in Portuguese.
[41] Vieira, L. S., Guedes, V. G., Matt, C. F., Cruz, M. E., and Castellões, F. V., 2007, "Integrated Thermoeconomic Optimization of a Benchmark Cogeneration System Using the Thermoflex Process Simulator," *Proceedings of the Eighth Iberoamerican Congress of Mechanical Engineering (CIBIM)*, Cusco, Peru, Paper No. 06-93, in Portuguese.
[42] Knight, R., Linder, U., Markworth, N., and Perz, E., 2004, "Thermo-Economic Optimization of Whole Gas Turbine Plant (GTPOM)," Appl. Therm. Eng., **24**(11–12), pp. 1725–1733.
[43] Díez, L. I., Cortés, C., and Campo, A., 2005, "Modelling of Pulverized Coal Boilers: Review and Validation of On-Line Simulation Techniques," Appl. Therm. Eng., **25**(10), pp. 1516–1533.
[44] Wei, D., Lu, X., Lu, Z., and Gu, J., 2008, "Dynamic Modeling and Simulation of an Organic Rankine Cycle (ORC) System for Waste Heat Recovery," Appl. Therm. Eng., **28**(10), pp. 1216–1224.
[45] van der Stelt, T., and Colonna, P., 2006, "FluidProp 2, What's New," Delft University of Technology, Delft, NL.
[46] SimTech Simulation Technology, 2000, "IPSEpro User Documentation-Version 3.1," Graz, AT.